Vibrational Spectroscopy xxx (xxxx) 103577

Contents lists available at ScienceDirect

Vibrational Spectroscopy

journal homepage: www.elsevier.com/locate/vibspec

High-pressure conformational and crystal polymorphs in 1-hexyl-3-methylimidazolium perfluorobutanesulfonate ionic liquid

Hiroshi Abe [a,*], Yoshihiro Koyama [b], Takahiro Takekiyo [c], Yukihiro Yoshimura [c]

[a] Department of Materials Science and Engineering, National Defense Academy, Hashirimizu 1-10-20, Yokosuka 239-8686, Japan
[b] Graduate School of Pure and Applied Science, University of Tsukuba, Tsukuba 305-8573, Japan
[c] Department of Applied Chemistry, National Defense Academy, Hashirimizu 1-10-20, Yokosuka 239-8686, Japan

ARTICLE INFO

Keywords:
Ionic liquid
Crystal polymorph
Conformational polymorph
Molecular packing
Conformational flexibility

ABSTRACT

An ionic liquid (IL) with conformational polymorphs indicated complicated phase transitions under high pressure (HP). The IL was 1-hexyl-3-methylimidazolium perfluorobutanesulfonate ([C_6mim][PFBS]), which has cationic and anionic conformational degrees of freedom. Using HP Raman spectroscopy, a competition between cation and anion conformers corresponded to the HP crystal polymorph. The folding cation appeared at 3.7 GPa due to its flexibility. The rigid [PFBS]$^-$ anion also formed the *gauche*‘ conformer at 7.6 GPa for higher packing efficiency. The conformational flexibility was adjusted depending on pressure. The pressure-variant/invariant conformations were connected with the HP crystal polymorph of [C_6mim][PFBS].

1. Introduction

Crystal polymorphs have been investigated related to packing and conformational polymorphs. Simple tetrahedra were used to simulate packing polymorphs depending on the packing fraction [1–3]. Orientational orders in various phases were sensitive to compression in the simulation box. In real molecular systems [4–9], molecular packing polymorphs were examined experimentally and theoretically, considering intermolecular interactions. The crystal packing arrangements determine the crystal structures. Moreover, molecular geometry-driven conformational polymorphs cause a variety of crystal structures [10,11]. By degrees of freedom of molecular conformations and their molecular flexibility, the crystal phases including metastable phases were selected at low temperature (LT) and high pressure (HP). Coupled with packing and conformational polymorphs, crystal polymorphs have been in progress in crystal science [12–16]. The idea of crystal energy landscape was introduced to interpret the experimentally obtained crystal polymorphs.

Ionic liquids (ILs) are regarded as a simple molecular system, that consists of a cation and an anion. The molecular conformations of cations and anions have been calculated with relating to the liquid and crystal structures of the ILs. Density functional theory (DFT) optimized the molecular conformations of the 1-alkyl-3-methylimidazolium ([$C_n$mim]$^+$) cations as representative cations [17–20], where n denotes the alkyl chain length. Using DFT, the potential energy surface was calculated to determine the stable conformations of [$C_n$mim]$^+$. In addition, some anions have conformational degrees of freedom. For instance, the perfluorobutanesulfonate ([$C_4F_9SO_3$]$^-$, [PFBS]$^-$) anion had two stable conformers, i.e., *trans* and *gauche* conformations [21]. The torsional potential of [PFBS]$^-$ is similar to that of [$C_4F_9BF_3$]$^-$ [22]. Experimentally, Raman bands can identify the molecular conformations. Cationic and anionic conformations are summarized in the literature [23].

Differential scanning calorimetry (DSC) was used to examine the LT phase behaviors of [$C_n$mim][PFBS] [24,25]. The LT crystal polymorphs of [C_6mim][PFBS] were detected on the DSC thermal traces. Further, simultaneous X-ray diffraction and DSC measurements were used to observe the LT crystal polymorphs in a series of [$C_n$mim][PFBS] (n = 4, 6, and 8) [21]. The LT crystal structures having large lattice constants were determined in [C_4mim][PFBS] and [C_8mim][PFBS]. Furthermore, using LT Raman spectroscopy, the cation and anion conformers of [$C_n$mim][PFBS] (n = 4, 6, and 8) were distinguished both upon cooling and heating [26]. The conformational changes at LT were related with the LT crystal polymorphs of the ILs. In addition, HP X-ray diffraction was conducted to compare the LT crystal polymorph of [C_4mim][PFBS] with the HP crystal polymorph. By HP Raman spectroscopy and HP X-ray diffraction, conformational changes of both cation and anion contributed to the crystal polymorph in [C_4mim][PFBS] [27]. The HP crystal polymorphs were entirely different from the LT ones. More importantly, HP X-ray diffraction was used to observe the reentrant layering

* Corresponding author.
E-mail address: ab@nda.ac.jp (H. Abe).

https://doi.org/10.1016/j.vibspec.2023.103577
Received 15 March 2023; Received in revised form 6 August 2023; Accepted 7 August 2023
0924-2031/© 20XX

in [C_6mim][PFBS] [28]. HP phase transition pathways were switched by the HP inherent layered structure. LT and HP crystal polymorphs of the ILs were summarized, combined with multiple phase transitions pathways [29–31].

In this study, HP Raman spectroscopy was used to examine HP conformational polymorphs of [C_6mim][PFBS]. HP inherent cationic and anionic conformers were directly determined, and the packing efficiency and conformational flexibility under HP was proceeded by the folding conformers both of cation and anion.

2. Materials and methods

[C_6mim][PFBS] (Kanto Chemical Co.) was the IL used in this study. Fig. 1 shows the molecular conformations of both [C_6mim]$^+$ and [PFBS]$^-$. The notations of n, t, g, and g' indicate *nonplanar, trans*, *gauche*, and *gauche*', respectively [20]. In a previous study [27], Raman spectroscopy assigned the *trans* and *gauche* conformers of [PFBS]$^-$.

A diamond anvil cell (DAC) was used to perform HP Raman spectroscopy. In a glovebox with dry flowing nitrogen, the sample and ruby balls were loaded into the hole (0.25 mm) of the pre-indented stainless gasket with a thickness of 0.18 mm in the DAC. An NRS-5100 Raman Spectrometer (JASCO Co.) equipped with a monochromator was used to obtain HP Raman spectra, and a Peltier-cooled camera was used for the measurements. A 5.8-mW green laser (wavelength of 532 nm) triggered the excitation.

DFT optimized the conformations of the cation and anion. In addition, DFT can identify Raman bands assigned to the molecular vibrations. The B3LYP hybrid functional and 6–31 + + G(d,p) basis set of the Firefly package (PC-GAMESS) was used to perform all DFT calculations [32,33].

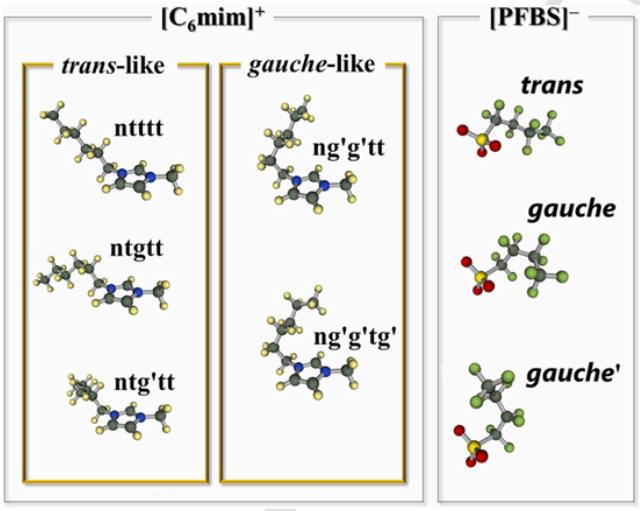

Fig. 1. Molecular conformers of [C_6mim]$^+$ and [PFBS]$^-$. n, t, g, and g' denote *nonplanar*, *trans*, *gauche*, and *gauche*', respectively.

3. Results

[C_6mim][PFBS] indicated HP crystal polymorphs and multiple pathways of phase transitions under HP by X-ray diffraction [28]. The HP crystal polymorph was different from the LT crystal polymorph [21]. In a previous study [28], the α and β phases possessed the layered structures (layering I) below 3.7 GPa (P_1), as shown in Fig. 2. Once the pressure exceeded 7.6 GPa (P_2), a different kind of hybrid layered structure (layering II, δ phase) was observed. It should be noticed that the space group of the [C_6mim][PFBS] crystals changed at P_1 and P_2 (Fig. 2).

Fig. 3 shows the Raman spectra upon compression in this study. In the same manner with LT [$C_n$mim][PFBS] in the previous study [26], an intermediate conformer, i, of [C_6mim]$^+$ was observed in the liquid (L) state. [C_6mim]$^+$ in the L phase provided the broad Raman bands, reflecting the dynamic fluctuations of the alkyl chain. Using the asymmetric pseudo-Voigt function [34], the asymmetric profile fitting was used to decompose the observed Raman bands. In case of the [PFBS]$^-$ anion at ambient pressure, t and g conformers coexisted at 382 cm^{-1} and 373 cm^{-1}, respectively.

In addition, the g' conformer of [PFBS]$^-$ was observed at 360 cm^{-1}, which was assigned by DFT (Fig. S1). It is emphasized that the bandwidths of [PFBS]$^-$ were narrower than those of [C_6mim]$^+$ (Fig. 3). Hence, the narrow Raman line widths of [PFBS]$^-$ even in the L phase imply that [PFBS]$^-$ behaves in the crystal circumstance. In fact, the line widths of [PFBS]$^-$ did not change at 0.3 GPa (P_C). At P_C, crystallization of the α phase (Fig. 2) was observed using an optical microscope. Clearly, Raman bands of both cation and anion changed drastically. The cation conformers were identified by referring to the previously observed LT Raman bands of [C_6mim][PFBS] [26]. Under HP, a *gauche*-like Raman band of [C_6mim]$^+$ was observed at ~600 cm^{-1} (Fig. 3), which was not detected at LT [26]. Using DFT (Fig. S2), the *gauche*-like Raman band was found to be ng'g'tt or ng'g'tg' (Fig. 1). This is a significant finding that the HP-inherent conformer is induced for higher packing efficiency. Furthermore, crystallization caused the conformational changes of [PFBS]$^-$. The peak intensities of the g and g' bands decreased remarkably at P_C. The g and g' bands almost disappeared at 0.6 GPa. In the crystal state, the t band of [PFBS]$^-$ was preferred for higher packing efficiency. As shown in Fig. 2, the α – β phase transition occurred without changing the space group at 1.7 GPa (P_0) [28]. It is noteworthy that, at $P_C < P < P_0$, the ntg'tt Raman intensity of [C_6mim]$^+$ decreased continuously upon compression (Fig. 3). Instead, the ntgtt band became larger with increasing pressure. This tendency opposed to temperature dependence of Raman spectra in LT [C_6mim][PFBS] [26]. Since the [PFBS]$^-$ anion indicated no pressure dependence in the α phase, conformations only of the cation were modified in the unit cell. Here, we emphasized that, by changing the cationic conformations, the packing efficiency of the α phase could be improved using the

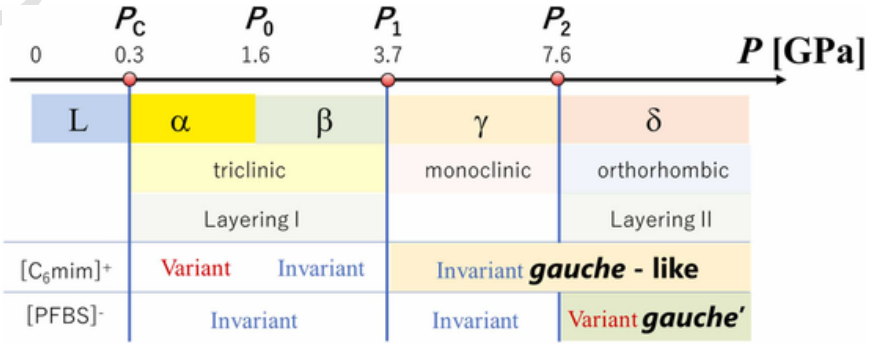

Fig. 2. Phase transitions and molecular conformers upon compression. X-ray diffraction determined the HP crystal structures of the α, β, γ, and δ phases [28].

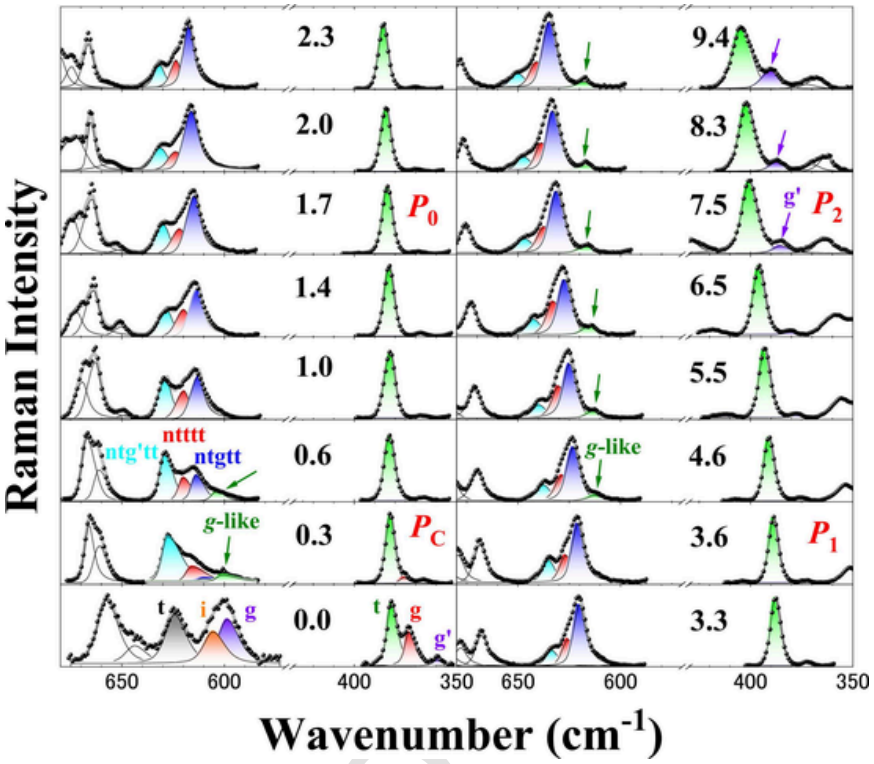

Fig. 3. Pressure dependence of Raman spectra of [C_6mim][PFBS] upon compression. The Raman bands of the cation and anion conformers appeared at 580–650 and 350–420 cm^{-1}, respectively. Raman spectra changed due to the high-pressure crystal polymorphs. The numbers in the figure indicate pressures (GPa).

flexible [C_6mim]$^+$. By further compression, the β phase appeared at P_0 (~ 1.7 GPa). The β phase existed below P_1 (=3.7 GPa) (Fig. 2). At $P_0 < P < P_1$, the conformational changes of both the cation and anion in the β phase were not observed at all (Fig. 3). Therefore, the β phase is expressed by the pressure-invariant conformers of the cation and anion. In this study, it was found that layering I at $P_C < P < P_1$ is formed by permitting the conformational changes (Fig. 3).

The additional Raman band of [C_6mim]$^+$ appeared at 613 cm^{-1} above P_1 (Fig. 3). The 613 cm^{-1} band at 4.6 GPa was small (Fig. 3). The weak band was equivalent to the *gauche*-like Raman band (ng'g'tt or ng'g'tg') of [C_6mim]$^+$ at 0.3 and 0.6 GPa. In the previous study [28], the space group change at P_1 was caused by the β – γ phase transition with disappearing layering I (Fig. 2). The structural feature of the γ phase was described by the small unit cell. The *gauche*-like conformer of the cation, as shown in Fig. 1, can explain the smaller unit cell of the γ phase [28]. As another example, in [C_4mim][PF_6], the folding conformer of [C_4mim]$^+$ easily lost the orientational orders, and a small unit cell was realized under HP [35]. In contrast, t of [PFBS]$^-$ was stable at $P_1 < P < P_2$. Compared with the flexible [C_6mim]$^+$ cation, the pressure-invariant [PFBS]$^-$ below P_2 is regarded as the rigid conformer. This HP behavior such as a flexible cation and a rigid anion was also seen in the previously observed HP phase transitions of [C_4mim][PFBS] [27]. At least, the relative flexibility and rigidity contributed to the HP crystal polymorphs both in [C_4mim][PFBS] and [C_6mim][PFBS].

Subsequently, the γ – δ phase transition at P_2 (~ 7.5 GPa) was also observed using Raman spectroscopy. In the previous study [28], it was clarified that the space group of the δ phase changed at P_2 and the unit cell became larger, accompanied with layering II (Fig. 2). More importantly, at P_2, the 382 cm^{-1} band of t conformer of [PFBS]$^-$ shifted to 401 cm^{-1} (Fig. 3). Moreover, the 360 cm^{-1} band of *gauche*-like conformer of [PFBS]$^-$ suddenly increased at P_2, and the peak shifted to 385 cm^{-1} (Fig. 3). The deference of the observed wavenumbers between t and *gauche*-like conformers was 16 cm^{-1} at P_2. Since the difference of the calculated one between t and g' was 17 cm^{-1} (Fig. S1), the *gauche*-like band was identified as the g' band. Nevertheless, the g' band was smaller than the t bands. A small portion of the folding [PFBS]$^-$ conformer was occupied in the δ phase. Simultaneously, peak broadening of the t band of [PFBS]$^-$ was predominant with the phase transition. The line broadening of all-*trans* conformation of [PFBS]$^-$ implied that the anionic alkyl chain is deformed for further molecular packing. Although the [PFBS]$^-$ conformers varied obviously at P_2, no spectral change was observed in [C_6mim]$^+$. This means that anion holding is indispensable due to the saturation of cation holding. Considering no reentrant layering of [C_4mim][PFBS] [27], we focus on the reentrant layering of [C_6mim][PFBS] from the viewpoint of the [PFBS]$^-$ folding. In the case of [C_4mim][PFBS], the intensity fraction of the g conformer of [PFBS]$^-$ reached 0.4 at 6.1 GPa [27]. In [C_6mim][PFBS], a small portion of both the folding cation and anion coexisted in the unit cell at P_2 (Fig. 2). Therefore, layering II originated from the main part of the *trans*-like conformers of [C_6mim]$^+$ and t conformer of [PFBS]$^-$. With increasing pressure in the δ phase, the bandwidth of [PFBS]$^-$ was enlarged, and the g' intensity increased gradually. The distorted t conformer and the increment of the g' conformer of [PFBS]$^-$ were related to the broadening of the *hk*0 Bragg reflections on the X-ray diffraction patterns [28]. The distorted and folding conformers caused the positional and orientational disorders on the (*hk*0) plane in the δ phase. Since the Raman bands were too broad above 11 GPa, the observed bans were not decomposed uniquely. In this study, the maximum pressure (P_{max}) was 13.5 GPa. Generally, polymerization [36] dissociation easily occurred under HP. Thus, it is important to confirm whether [C_6mim][PFBS] recovered or not after compression up to P_{max}. Thus, we gradually decreased the pressure. Finally, the sample returned to the L phase at ambient pressure. Fig. S3 shows the Raman spectra before/after compression. Judging from almost the same Raman spectra before/after compression, it was found that the sample completely recovered without polymerization or dissociation.

Quantitative conformational analysis provides the detailed molecular behaviors for further discussion. Fig. 4(a) shows the pressure depen-

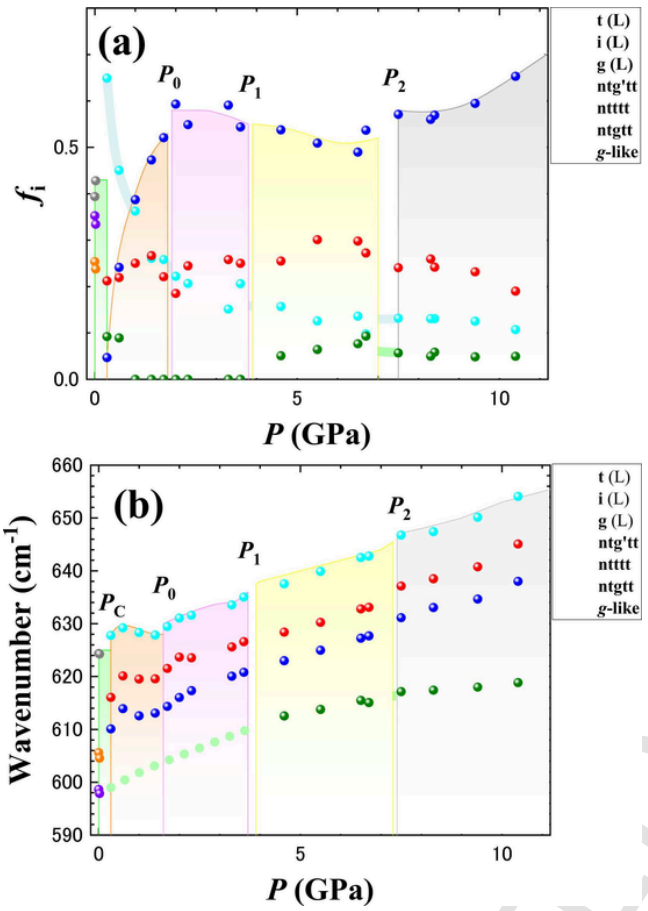

Fig. 4. Pressure dependences of (a) intensity fractions, f_i, and (b) band positions of $[C_6mim]^+$ upon compression.

dence of the conformational ratios of $[C_6mim]^+$. The intensity fraction, f_i, of the $[C_6mim]^+$ conformer is provided by,

$$f_i = \frac{I_i}{I_{ntg'tt} + I_{ntttt} + I_{ntgtt} + I_{g-like}} \quad (1)$$

where $I_{g\text{-like}}$ is the Raman intensity of the *gauche*-like conformer (ng'g'tt or ng'g'tg'). Pressure dependences of f_i were obtained by profile fitting. Fig. 4(a) clearly plots the pressure variant/invariant properties of $[C_6mim]^+$. At P_C, the molecules were loosely packed in the low symmetry crystal. During the α phase at $P_C < P < P_0$, the f_{ntgtt} increased, and $f_{ntg'tt}$ decreased drastically while preserving the crystal structure. The crossover behavior in the α phase indicates that the conformational changes of flexible $[C_6mim]^+$ are valid for more densely packing. In the P_0 vicinity, the packing efficiency reached the limit only by the conformational changes. The α – β phase transition at P_0 improved the molecular packing by the molecular rearrangement. In the β phase, the cationic and anionic conformational changes were suppressed, and layering I was maintained with increasing the structural strain. However, at P_1, layering I collapsed, and a new monoclinic crystal structure was initiated by the molecular rearrangement. Moreover, the *gauche*-like conformer of $[C_6mim]^+$ was formed for the more compact packing above P_1 (Fig. 4(a)). As shown in Fig. 3, the band broadening of the *trans*-based conformers above P_1 corresponds to the static disorder of the conformers, resembling the dynamic disorder expressed by the broad band in the L phase. More importantly, at P_2, the orthorhombic lattice with the larger unit cell was induced to shuffle the molecular packing state. In the δ phase, the gradual increment of the f_{ntgtt} in Fig. 4 (a) is connected with the mutual alkyl chain packing of $[C_6mim]^+$, which is indispensable for the two-dimensional layering II. In contrast, Fig. 4(b) plots the pressure dependence of band positions of the $[C_6mim]^+$ conformers. The band position of the *gauche*-like conformer of $[C_6mim]^+$ above P_1 is linked with the *gauche* conformer in the L phase (Fig. 4(b)). Generally, the wavenumber slope change as a function of pressure indicates the molecular stiffening. In the α phase, softening occurred due to the distinct conformational changes of $[C_6mim]^+$, as mentioned earlier (Fig. 4(a)). Above P_1, a monotonic shifting of the Raman bands of $[C_6mim]^+$ was observed with increasing pressure. It should be noticed that the slope of *gauche*-like conformer is relatively small. Thus, the hardening t conformer and relatively softening g-like conformer coexisted above P_1. In the unit cell, the locally softening g-like conformer of $[C_6mim]^+$ plays an important role in tuning the packing efficiency.

The next step is to clarify the $[PFBS]^-$ conformational behaviors under HP relating to the crystal polymorph. Similar to the cationic f_i, the anionic f_i in the α phase depended extensively on the pressure (Fig. 5 (a)). For instance, the g and g' conformers decreased, while the t conformer increased. Simultaneously, a bending pressure point of the wavenumber slopes appeared at P_0 (Fig. 5(b)). Considering both f_i and band shifting as a function of pressure, the HP behaviors of $[PFBS]^-$ in the α phase at $P_C < P < P_0$ were different from those at the other pressure regions. Pressure-variant f_i and low slope of band shifting below P_0 imply that the relatively soft conformers of $[PFBS]^-$ are alternated rather than conformational hardening. Since the wavenumber slopes became larger discontinuously above P_0, conformational hardening of the $[PFBS]^-$ occurred. At $P_0 < P < P_2$, the f_t and $f_{g'}$ of $[PFBS]^-$ were almost constant on the pressure scale. Hence, the $[PFBS]^-$ conformers did not contribute to the β and γ phases. On the contrary, above P_2, $f_{g'}$ of

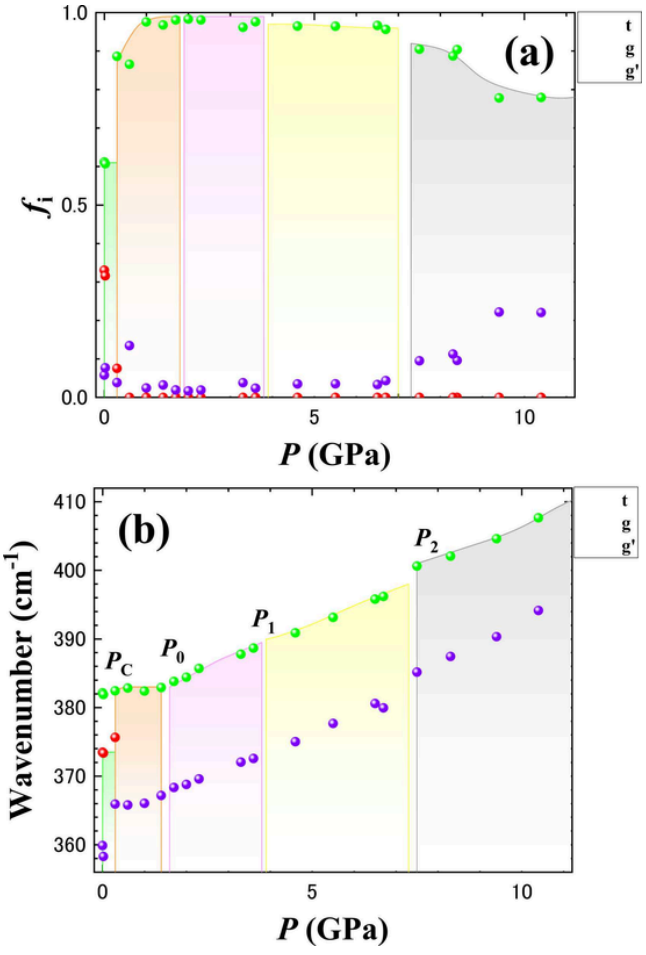

Fig. 5. Pressure dependences of (a) intensity fractions, f_i, and (b) band positions of $[PFBS]^-$ upon compression.

[PFBS]− increased during layering II (Fig. 5(a)). Here, it is emphasized that two conditions are proposed for more densely packing; one is conformational changes, and the other is molecular rearrangement using a phase transition. Two conditions, i.e., molecular shuffling and [PFBS]− folding, occurred simultaneously at P_2 due to a smaller void space in the δ phase. Combined with the cationic behaviors, in [C_6mim][PFBS], more dense packing above P_2 could be realized by a combination of the molecular conformational changes (cationic f_{ntgtt} and anionic $f_{g'}$) and phase transitions with the molecular rearrangement.

4. Conclusions

Raman spectroscopy was used to examine the HP-inherent conformer relating to the HP crystal polymorph. The *gauche*-like conformer of [C_6mim]$^+$ was formed only under HP. The cationic and anionic conformations changed at the phase transition pressures. Layering I at $P_C < P < P_1$ (α phase) was formed mainly by the *trans*-based conformer, and the flexible cation in the α phase can change their conformations depending on pressure. The layered structure collapsed due to the reappearance of the *gauche*-like conformers of [C_6mim]$^+$ at P_1. Pressure-invariant [PFBS]− conformers suggest that [C_6mim]$^+$ is more flexible than [PFBS]−. Layering II (δ phase) appeared at P_2, and the cationic *trans*-like and anionic folding g' conformers increased due to a small amount of void volume in the δ phase. Using Raman spectroscopy, the conformational flexibility in [C_6mim][PFBS] was clarified under HP. The pressure-variant/invariant conformers in the well-packed circumstance can explain the complicated HP crystal polymorph of [C_6mim][PFBS].

CRediT authorship contribution statement

Hiroshi Abe: Conceptualization; Roles/Writing - original draft; Writing - review & editing, Yoshihiro Koyama: Data curation, Takahiro Takekiyo: Data curation, Yukihiro Yoshimura: Supervision, The statements were agreed by all authors.

Declaration of Competing Interest

There are no conflicts to declare.

Data availability

Data will be made available on request.

Acknowledgments

The authors thank Dr. H. Kishimura of the National Defense Academy and Prof. N. Hamaya of Ochanomizu University for their helpful discussions.

Appendix A. Supporting information

Supplementary data associated with this article can be found in the online version at doi:10.1016/j.vibspec.2023.103577.

References

[1] A. Haji-Akbari, M. Engel, A.S. Keys, X. Zheng, R.G. Petschek, P. Palffy-Muhoray, S.C. Glotzer, Disordered, quasicrystalline and crystalline phases of densely packed tetrahedra, Nature 462 (2009) 773–777.
[2] R. van Damme, G.M. Coli, R. van Roij, M. Dijkstra, Classifying crystals of rounded tetrahedra and determining their order parameters using dimensionality reduction, ACS Nano 14 (2020) 15144–15153.
[3] K. Je, S. Lee, E.G. Teich, M. Engel, S.C. Glotzer, Entropic formation of a thermodynamically stable colloidal quasicrystal with negligible phason strain, Proc. Nat. Acad. Soc. 118 (2021) e2011799118–7.
[4] R.K. Kamlekar, M.J. Swamy, Molecular packing and intermolecular interactions in two structural polymorphs of N-palmitoylethanolamine, a type 2 cannabinoid receptor agonist, J. Lipid Res. 47 (2006) 1424–1433.
[5] X. He, A.C. Benniston, H. Saarenp¨a¨a, H. Lemmetyinen, N.V. Tkachenko, U. Baisch, Polymorph crystal packing effects on charge transfer emission in the solid state, Chem. Sci. 6 (2015) 3525–3532.
[6] K.M. Steed, J.W. Steed, Packing problems: high Z′ crystal structures and their relationship to cocrystals, inclusion compounds, and polymorphism, Chem. Rev. 115 (2015) 2895–2933.
[7] A.O. Surov, A.N. Manin, A.P. Voronin, A.V. Churakov, G.L. Perlovich, M.V. Vener, Weak interactions cause packing polymorphism in pharmaceutical two-component crystals. The case study of the salicylamide cocrystal, Cryst. Growth Des. 17 (2017) 1425–1437.
[8] B.A. Nogueira, C. Castiglioni, R. Fausto, Color polymorphism in organic crystals, Commun. Chem. 3 (2020) 34–12.
[9] G.H. Roche, D. Flot, J.J.E. Moreau, O.J. Dautel, J.-S. Filhol, A. van der Lee, Packing polymorphism affecting the optoelectronic properties of a π-conjugated organic compound, Cryst. Growth Des. 21 (2021) 3850–3863.
[10] A.J. Cruz-Cabeza, J. Bernstein, Conformational polymorphism, Chem. Rev. 114 (2014) 2170–2191.
[11] M. Mortazavi, J. Hoja, L. Aerts, L. Quéré, J. van de Streek, M.A. Neumann, A. Tkatchenko, Computational polymorph screening reveals late-appearing and poorly-soluble form of rotigotine, Commun. Chem. 2 (2019) 70–77.
[12] S.L. Price, From crystal structure prediction to polymorph prediction: interpreting the crystal energy landscape, Phys. Chem. Chem. Phys. 10 (2008) 1996–2009.
[13] S.Z. Ismail, C.L. Anderton, R.C.B. Copley, L.S. Price, S.L. Price, Evaluating a crystal energy landscape in the context of industrial polymorph screening, Cryst. Growth Des. 13 (2013) 2396–2406.
[14] S.L. Price, D.E. Braun, S.M. Reutzel-Edens, Can computed crystal energy landscapes help understand pharmaceutical solids? Chem. Commun. 52 (2016) 7065–7077.
[15] G.J.O. Beran, Modeling polymorphic molecular crystals with electronic structure theory, Chem. Rev. 116 (2016) 5567–5613.
[16] A.J. Cruz-Cabeza, N. Feeder, R.J. Davey, Open questions in organic crystal polymorphism, Commun. Chem. 3 (2020) 142–144.
[17] J.N. Canongia Lopes, J. Deschamps, A.A.H. Pa´dua, Modeling ionic liquids using a systematic all-atom force field, J. Phys. Chem. B 108 (2004) 2038–2047.
[18] S. Tsuzuki, A.A. Arai, K. Nishikawa, Conformational analysis of 1-butyl-3-methylimidazolium by CCSD(T) level Ab initio calculations: effects of neighboring anions, J. Phys. Chem. B 112 (2008) 7739–7747.
[19] J. Kiefer, C.C. Pye, Structure of the room-temperature ionic liquid 1-hexyl-3-methylimidazolium hydrogen sulfate: conformational isomerism, J. Phys. Chem. A 114 (2010) 6713–6720.
[20] T. Endo, T. Higuchi, Y. Kimura, DFT study on conformation of 1-alkyl-3-methylimidazolium with ethyl, propyl, butyl, pentyl, and hexyl group, Bull. Chem. Soc. Jpn. 93 (2020) 720–729.
[21] Y. Koyama, S. Shimono, H. Abe, K. Matsuishi, Crystal polymorphs in 1-alkyl-3-methylimidazolium perfluorobutanesulfonate ionic liquids, J. Mol. Liq. 317 (2020) 113908-7.
[22] S. Tsuzuki, T. Umecky, H. Matsumoto, W. Shinoda, M. Mikami, Interactions of perfluoroalkyltrifluoroborate anions with li ion and imidazolium cation: effects of perfluoroalkyl chain on motion of ions in ionic liquids, J. Phys. Chem. B 114 (2010) 11390–11396.
[23] V.H. Paschoal, L.F.O. Faria, M.C.C. Ribeiro, Vibrational spectroscopy of ionic liquids, Chem. Rev. 117 (2017) 7053–7112.
[24] A.B. Pereiro, M.J. Pastoriza-Gallego, K. Shimizu, I.M. Marrucho, J.N. Canongia Lopes, M.M. Piñeiro, L.P.N. Rebelo, On the formation of a third, nanostructured domain in ionic liquids, J. Phys. Chem. B 117 (2013) 10826–10833.
[25] M.L. Ferreira, M.J. Pastoriza-Gallego, J.M.M. Araújo, J.N. Canongia Lopes, L.P.N. Rebelo, M.M. Piñeiro, K. Shimizu, A.B. Pereiro, Influence of nanosegregation on the phase behavior of fluorinated ionic liquids, J. Phys. Chem. C. 121 (2017) 5415–5427.
[26] H. Abe, H. Kishimura, M. Uruichi, A phase variety of fluorinated ionic liquids: Molecular conformational and crystal polymorph, Spectrochim. Acta A 286 (2023) 121948–7.
[27] Y. Koyama, S. Shimono, H. Kishimura, T. Takekiyo, Y. Yoshimura, H. Abe, K. Matsuishi, High-pressure crystal polymorphs in 1-butyl-3-methylimidazolium perfluorobutanesulfonate, J. Mol. Liq. 335 (2021) 116415–116417.
[28] H. Abe, Y. Koyama, S. Shimono, H. Kishimura, K. Matsuishi, High-pressure crystal polymorphs and multiple pathways in 1-hexyl-3-methylimidazolium perfluorobutanesulfonate ionic liquid, Chem. Phys. 557 (2022) 111479–7.
[29] H. Abe, H. Kishimura, T. Takekiyo, Y. Yoshimura, N. Hamaya, Non-equilibrium protic and aprotic ionic liquids: Measuring the distance from the equilibrium state, J. Mol. Liq. 283 (2019) 196–207.
[30] H. Abe, H. Kishimura, T. Takekiyo, T. Hanasaki, Y. Yoshimura, N. Hamaya, Low-temperature and high-pressure phase changes of room temperature ionic liquids, J. Mol. Liq. 300 (2020) 112340–112349.
[31] H. Abe, Phase variety in ionic liquids: hydrogen bonding and molecular conformations, J. Mol. Liq. 332 (2021) 115189-27.
[32] A.A. Granovsky, Firefly version 8, http://classic.chem.msu.su/gran/firefly/index.html.
[33] M.W. Schmidt, K.K. Baldridge, J.A. Boatz, S.T. Elbert, M.S. Gordon, J.H. Jensen, S. Koseki, N. Matsunaga, K.A. Nguyen, S. Su, T.L. Windus, M. Dupuis, J.A. Montgomery Jr, General atomic and molecular electronic structure system, J. Comput. Chem. 14 (1993) 1347–1363.
[34] V.I. Korepanov, D.M. Sedlovets, An asymmetric fitting function for condensed-phase Raman spectroscopy, Analyst 143 (2018) 2674–2679.

[35] H. Abe, T. Takekiyo, N. Hatano, M. Shigemi, N. Hamaya, Y. Yoshimura, Pressure-induced Frustration–Frustration process in 1–butyl-3-methylimidazolium hexafluorophosphate, a room-temperature ionic liquid, J. Phys. Chem. B 118 (2014) 1138–1145.

[36] F. Chen, T. You, Y. Yuan, C. Pei, X. Ren, Y. Huang, Z. Yu, X. Li, H. Zheng, Y. Pan, K. Yang, L. Wang, Pressure-induced structural transitions of a room temperature ionic liquid—1-ethyl-3-methylimidazolium chloride, J. Chem. Phys. 146 (2017) 094502–094510.